

# Three-Dimensional Rayleigh-Bénard Convection of a Rarefied Gas: DSMC and Navier-Stokes Calculations

S. K. Stefanov<sup>\*</sup>, V. M. Roussinov<sup>\*</sup>, C. Cercignani<sup>\*\*</sup>

<sup>\*</sup>*Institute of Mechanics, BASci., Acad. G. Bonchev Str., Block. 4, 1113 Sofia Bulgaria*

<sup>\*\*</sup>*Dipartimento di Matematica, Politecnico di Milano, p.zza L. da Vinci, 32, 20133 Milan, Italy*

**Abstract.** The three-dimensional Rayleigh-Bénard convection of a rarefied gas is studied numerically by using DSMC and Navier-Stokes finite difference methods. We present the results obtained in a three-dimensional box with an aspect ratio  $A=L_x:L_y:L_z$  at a fixed wall temperature ratio  $r=T_c/T_h=0.1$ . In general, the three-dimensional results confirm the validity of the zone of convection obtained in the previous author's two-dimensional considerations [1,2]. A detailed analysis has been performed for Knudsen number  $Kn=0.02$  and  $A=2:2:1$ ,  $A=3:3:1$ , and  $A=4:4:1$  and different Froude numbers ranged within the zone of convection. As result, a variety of different stable convection patterns in form of rolls and squares has been obtained. For the lowest Knudsen numbers computed,  $Kn=0.001$  and  $Kn=0.002$ , Froude number  $Fr=1.0$ , and a fixed aspect ratio  $A=2:2:1$ , an irregular (chaotic) flow in form of unstable polygonal patterns has been observed.

## INTRODUCTION

The formation and development of convection flows in a fluid confined between two horizontal parallel plates with the bottom plate heated from below is a classical problem known as the Rayleigh-Bénard problem. In our previous papers [1, 2] we have studied the formation of convection patterns in the Rayleigh-Bénard (RB) flow of a rarefied gas in a rectangular two-dimensional domain by using two different numerical approaches: particle simulation by the DSMC method and Navier-Stokes finite difference (FD) calculations. The calculations have been performed within a range of Knudsen number  $Kn = 0.001-0.04$  and Froude number  $Fr=0.5-1.5 \times 10^3$  and a fixed temperature ratio  $r=0.1$ . We have observed a variety of possible final states (attractors), namely: pure heat conduction, stable vortex roll convection, periodic, wavy, and chaotic regimes.

In the present paper we extend the study of the problem to convection gas flows in a three-dimensional box. The low Knudsen numbers allow again the problem to be investigated by using two numerical approaches: DSMC method (particle approach) and finite difference method (continuum approach based on the model of compressible viscous heat conducting gas with state-dependent transport coefficients). Using the DSMC method, the three-dimensional convection of a rarefied gas has been investigated by Watanabe [3] for the case of a hypothetical value of the gravitational acceleration (the Froude number in non-dimensional formulation) so as to minimize the density variation in the pure heat conduction state. The same approach, imitating the conditions of the Boussinesq approximation (valid for continuum fluid dynamics), has been used previously by Garcia *et al.* [4] and Watanabe *et al.* [5] for the two-dimensional case of convection in rarefied gas. In our calculations, the governing non-dimensional parameter  $Fr$  was varied freely so strongly stratified states could be investigated. This idea was proposed by Stefanov and Cercignani [6] and used by Sone *et al.* [7], Stefanov *et al.* [1,2] for a detailed investigation of the two-dimensional Rayleigh-Bénard problem of a rarefied gas. In the present paper we follow that second approach and investigate the three-dimensional RB flow for a set of  $Kn$  and  $Fr$  at fixed temperature ratio  $r=0.1$ . The dependence of the pattern formation on the aspect ratio  $A = L_x:L_y:L_z$  is also studied. The most detailed analysis is performed for  $Kn=0.02$ ,  $Fr=3.0$  and aspect ratios  $A=2:2:1$ ,  $A=3:3:1$  and  $A=4:4:1$ . For the same  $Kn=0.02$  and aspect ratios  $A=2.0$  and  $A=3.0$  the calculation are performed for  $Fr=1.5$ ,  $Fr=3.0$  and  $Fr=7.0$ . The next computations have been performed for sufficiently low Knudsen numbers  $Kn=0.002$  and  $Kn=0.001$ , where one can expect development of more complicated flow regimes, as was discovered in [1,2] for the two-dimensional RB flow.

Report Documentation Page				Form Approved OMB No. 0704-0188	
Public reporting burden for the collection of information is estimated to average 1 hour per response, including the time for reviewing instructions, searching existing data sources, gathering and maintaining the data needed, and completing and reviewing the collection of information. Send comments regarding this burden estimate or any other aspect of this collection of information, including suggestions for reducing this burden, to Washington Headquarters Services, Directorate for Information Operations and Reports, 1215 Jefferson Davis Highway, Suite 1204, Arlington VA 22202-4302. Respondents should be aware that notwithstanding any other provision of law, no person shall be subject to a penalty for failing to comply with a collection of information if it does not display a currently valid OMB control number.					
1. REPORT DATE <b>13 JUL 2005</b>		2. REPORT TYPE <b>N/A</b>		3. DATES COVERED <b>-</b>	
4. TITLE AND SUBTITLE <b>Three-Dimensional Rayleigh-Bénard Convection of a Rarefied Gas: DSMC and Navier-Stokes Calculations</b>				5a. CONTRACT NUMBER	
				5b. GRANT NUMBER	
				5c. PROGRAM ELEMENT NUMBER	
6. AUTHOR(S)				5d. PROJECT NUMBER	
				5e. TASK NUMBER	
				5f. WORK UNIT NUMBER	
7. PERFORMING ORGANIZATION NAME(S) AND ADDRESS(ES) <b>Institute of Mechanics, BASci., Acad. G. Bonchev Str., Block. 4, 1113 Sofia Bulgaria</b>				8. PERFORMING ORGANIZATION REPORT NUMBER	
9. SPONSORING/MONITORING AGENCY NAME(S) AND ADDRESS(ES)				10. SPONSOR/MONITOR'S ACRONYM(S)	
				11. SPONSOR/MONITOR'S REPORT NUMBER(S)	
12. DISTRIBUTION/AVAILABILITY STATEMENT <b>Approved for public release, distribution unlimited</b>					
13. SUPPLEMENTARY NOTES <b>See also ADM001792, International Symposium on Rarefied Gas Dynamics (24th) Held in Monopoli (Bari), Italy on 10-16 July 2004.</b>					
14. ABSTRACT					
15. SUBJECT TERMS					
16. SECURITY CLASSIFICATION OF:			17. LIMITATION OF ABSTRACT <b>UU</b>	18. NUMBER OF PAGES <b>6</b>	19a. NAME OF RESPONSIBLE PERSON
a. REPORT <b>unclassified</b>	b. ABSTRACT <b>unclassified</b>	c. THIS PAGE <b>unclassified</b>			

In general, the analysis of the obtained results for the three-dimensional Rayleigh-Bénard flow show that the zone of governing parameters, in which a transition from pure heat conduction to the regime of convection takes place, is in good agreement with the zone delineated by the two-dimensional calculations [1]. A chaotic convection in form of different unstable polygonal patterns has been obtained within the range of Knudsen numbers  $Kn=0.001-0.002$  and a Froude number around  $Fr=1.0-1.1$ . For larger  $Kn$  and  $Fr$  we have observed a variety of stable structures in form of roll or square patterns.

## Problem Formulation And Computational Considerations

The three-dimensional Rayleigh-Bénard problem for a rarefied gas treats a monatomic simple gas with average number density  $n_0$  studied in a rectangular computational domain  $D(L_x \times L_y \times L_z)$  i.e. with an aspect ratio  $A=L_x/L_z, L_y/L_z$ . The domain is confined in the vertical  $z$ -direction by two diffusely reflecting horizontal walls (the lower wall temperature is greater than the upper one,  $T_h > T_c$ ) and a periodic boundary condition is implemented in the horizontal  $x$ - and  $y$ -directions at vertical planes at mutual distances  $L_x$  and  $L_y$ . A constant acceleration  $\mathbf{g}=(g_x, g_y, g_z)=(0, 0, -g)$  acts on the gas in each point of the computational domain. A hard sphere molecular model is employed in the simulation of binary collisions. The governing nondimensional parameters are the Knudsen number  $Kn=\ell_0/L_z$ , the Froude number  $Fr=V_{th}^2/gL_z$ , and the temperature ratio  $\tau=T_h/T_c$ , where  $\ell_0$  is mean free path in a “hard sphere” gas with density  $n_0$ , and  $V_{th}$  is the most probable molecular velocity in equilibrium gas with temperature  $T_h$ . In our consideration all variables are normalized by using the following scales: for density,  $\rho_0=mn_0$  ( $m$  is the molecular mass); for velocity,  $V_{th}$ ; for length, the distance  $L_z$ ; for time,  $t_0=L_z/V_{th}$ ; for temperature,  $T_h$ .

The time evolution of this system when starting from a certain initial state has been studied by means of the two approaches discussed in the introduction: molecular and continuum.

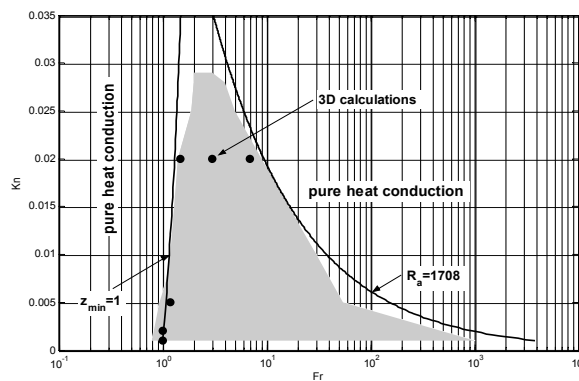
The DSMC technique uses a finite number of model particles that move and collide in the three-dimensional space domain  $D$  to perform a direct simulation of the molecular gas dynamics. The algorithm follows the basic steps of the “No Time Counter” scheme suggested by Bird [8]. A uniform rectangular basic grid with  $N_x \times N_y \times N_z$  cells covers the computational domain. Within every time step each basic cell is subdivided dynamically into subcells in order to meet the special resolution requirements; the size of a subcell is less than the local mean free path. In this way, only the information about the basic grid is kept permanently in the computer memory. The sampling is conducted on a coarser grid with larger cells containing a group of basic cells. This multilevel grid scheme allows a correct calculation of the molecular process on an adaptive fine grid and at the same time provides a meaningful sample size of the instantaneous macroscopic variables by averaging simultaneously over a group of cells. For example, for  $Kn=0.02$  and  $A=2:2:1$  a grid with  $100 \times 100 \times 50$  basic cells is used; while for  $Kn=0.02$  and  $A=4:4:1$  –  $200 \times 200 \times 50$ . For the computed lower  $Kn=0.002$  the grid at  $A=2:2:1$  is with  $200 \times 200 \times 100$  basic cells. The instantaneous fields are sampled by time averaging over 500 time steps  $\Delta t$  ( $\Delta t$  is less than mean collision time). Finally, the obtained three-dimensional instantaneous macroscopic fields are processed by a simple average filter in order to remove the high-frequency statistical fluctuations from the simulation results. Depending on the Knudsen number and the aspect ratio  $A$  the total number of model particles varies from  $5 \times 10^6$  to  $32 \times 10^6$ .

The 3D finite difference (FD) calculations of the continuum model based on the Navier-Stokes equations for a compressible viscous gas with state dependent transport coefficients (see [1]) are performed by using an implicit conservative finite difference (second order in space and first order in time) scheme with inner iteration process within each time step. During each iteration a 7-bandmatrix linear equation system obtained for each macroscopic variable is solved by using a generalized conjugate gradient (GCG) method. The iteration error is chosen to be not larger than  $10^{-10} - 10^{-11}$  depending on the chosen computational parameters of the scheme. The size of the rectangular uniform computational grid depends on the Knudsen number and the aspect ratio  $A$ . For the most difficult cases,  $Kn=0.002$  and  $Kn=0.001$  at fixed aspect ratio  $A=2.0$ , a grid with  $200 \times 200 \times 100$  nodes is used. For the larger  $Kn=0.02$  the calculations are performed on grids  $100 \times 100 \times 50$ ,  $150 \times 150 \times 50$ , and  $200 \times 200 \times 50$  for aspect ratios  $A=2.0$ ,  $A=3.0$ , and  $A=4.0$ , respectively.

## Numerical Results

We illustrate the obtained results using a limited set of the computational data. In our previous works [1,2] we have shown that the two-dimensional calculations of the RB flow, performed by using both molecular and continuum approach for the range of the governing parameters mentioned in the introduction, exhibited a qualitative and quantitative similarity of the obtained convective flows. That is why, here our main goal is not to present a detailed comparison of both model calculations for the three-dimensional case of RB flow but to use each of the two

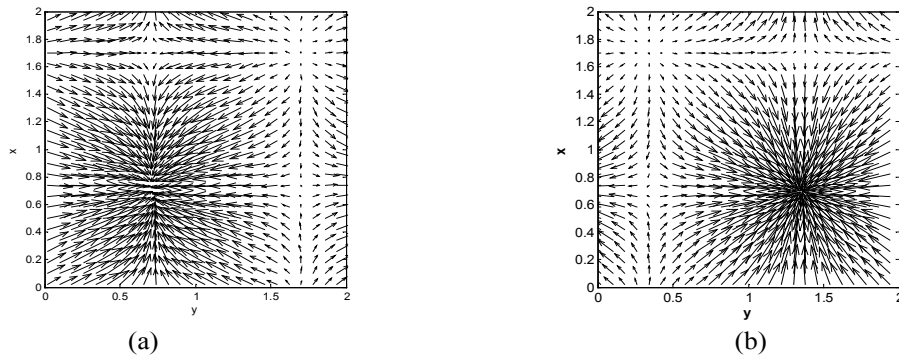
models where it is more effective in order to cover a wider range of the parameters where new interesting convection phenomena might exist. A rough preliminary comparative analysis has convinced us that we could not expect great surprises and both models should give similar results within the studied range of the parameters. This work is in progress and a more detailed discussion on the comparison of the two models in the three-dimensional case of the RB convection will be given in a separate paper. Here we follow the line of presenting our results for a set of calculations performed by using the DSMC simulations for  $Kn=0.02$  and various  $Fr$  and aspect ratios where the particle method was more effective than the finite difference computations. In the cases with a smaller Knudsen number,  $Kn=0.002$  and  $0.001$ , the FD method was considerably more effective because it turned out possible to obtain a quantitatively correct results on sufficiently coarser grid than a grid that meets the computational requirements of the DSMC method. Thus, the results presented here for the chaotic convection at  $Kn=0.002$  and  $Fr=1.0$  were computed by using the FD method. This case was run by DSMC within the initial part of the transient period where the results were similar to those obtained by FD. For the comparative analysis in this case, the DSMC calculations will be continued beyond the transient period.



**FIGURE 1.** The zone of convection and the points of the three-dimensional computations: the analytical conditions for the left and right boundaries of the zone of convection [1], are given with solid lines, the gray shaded zone illustrates the two-dimensional calculations [1,2], the three-dimensional calculations are given with filled circles.

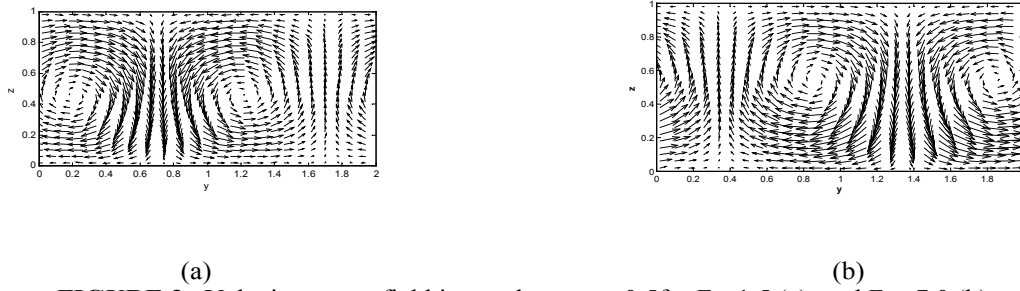
Figure 1 shows the points (filled circles) of the three-dimensional calculations in a coordinate system of  $Fr$  and  $Kn$  numbers (the temperature ratio is fixed  $r=0.1$ ). The gray shaded polygon illustrates the zone of convection obtained from the two-dimensional calculations [1]. The analytical conditions for the left and right boundaries of the zone of convection ( eqs. (15) and (16) in [1]) are shown by solid lines. Additionally, several 3D calculations have been performed for points outside of the delineated zone of convection but close enough to its boundaries. In general, these 3D-runs, performed by using DSMC method for  $Kn=0.02$  and  $Kn=0.01$ , confirmed the two-dimensional results [1] obtained for the boundaries of the zone of convection.

Figures 2 and 3 illustrate the convection patterns for fixed  $Kn=0.02$  and  $A=2.0$  at  $Fr=1.5$  (a) ( the left side



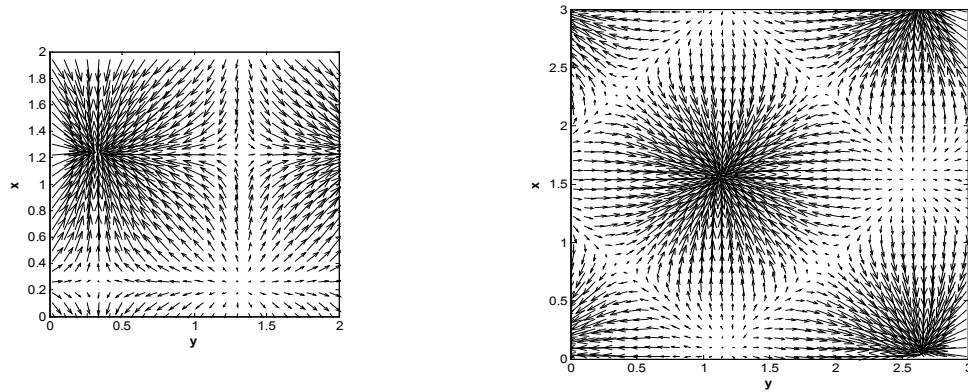
**FIGURE 2.** Velocity vector field in  $xy$ -plane at  $z=0.9$  for  $Kn=0.02$ ,  $A=2$ , and  $Fr=1.5$  (a) ,  $Fr=7.0$  (b).

of the convection zone where gravity prevails against the temperature gradient action) and at  $Fr=7.0$  ( the right side, where the temperature gradient is dominating). The “view from above” at  $z=0.9$  (Fig. 2) showed that in both cases the convection flow is organized as an asymmetrically positioned single square cell with a single sink point (the focal point of the velocity vectors). Figure 3 shows the similar vortex configuration in a vertical plane section at  $x=0.5$  in cases (a) and (b) as defined in Figure 2. From the figure one can see that the vortex center is shifted up with the increase of the Froude number.

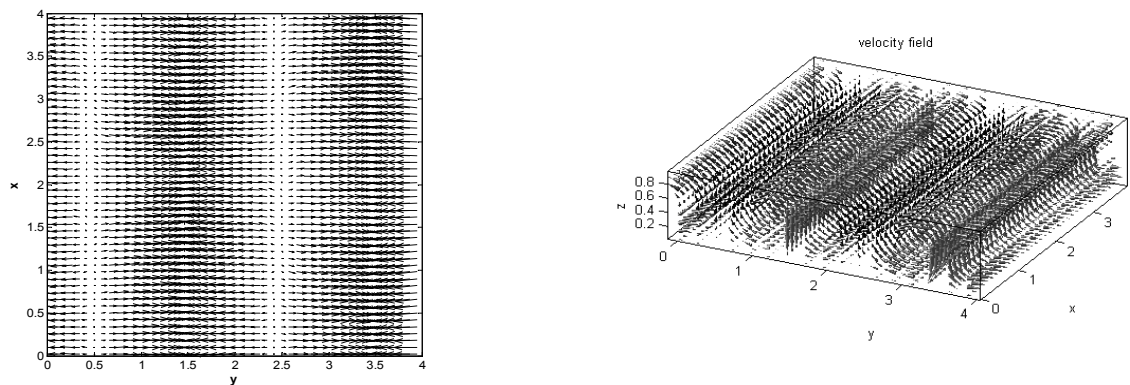


**FIGURE 3.** Velocity vector field in  $yz$ -plane at  $x=0.5$  for  $Fr=1.5$  (a) and  $Fr=7.0$  (b)

Figures 4 and 5 show the flow patterns for different aspect ratios  $A=2$ ,  $A=3$ , and  $A=4$  at  $Kn=0.02$  and  $Fr=3.0$ .

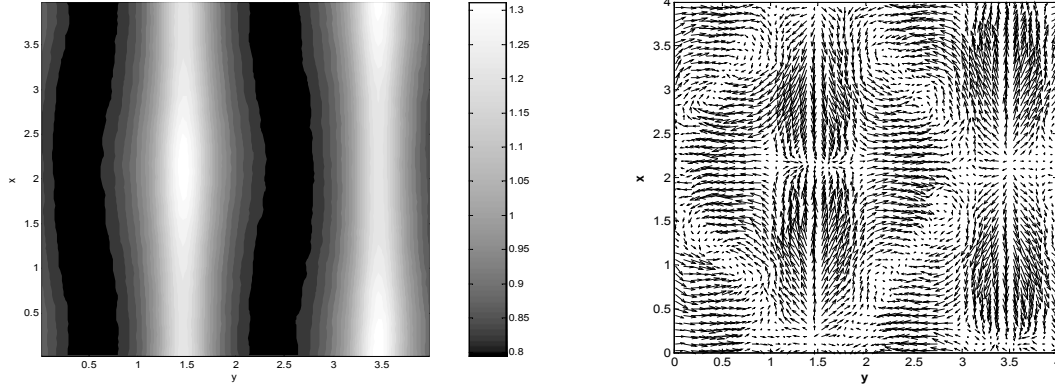


**FIGURE 4.** Velocity vector field in  $xy$ -plane at  $z=0.9$  for  $Kn=0.02$ ,  $Fr=3.0$  and aspect ratios  $A=2$  (left),  $A=3$  (right)



**FIGURE 5.** Velocity vector field in  $xy$ -plane at  $z=0.9$  (left) and 3D velocity vector plot for  $Kn=0.02$ ,  $Fr=3.0$ ,  $A=4.0$ .

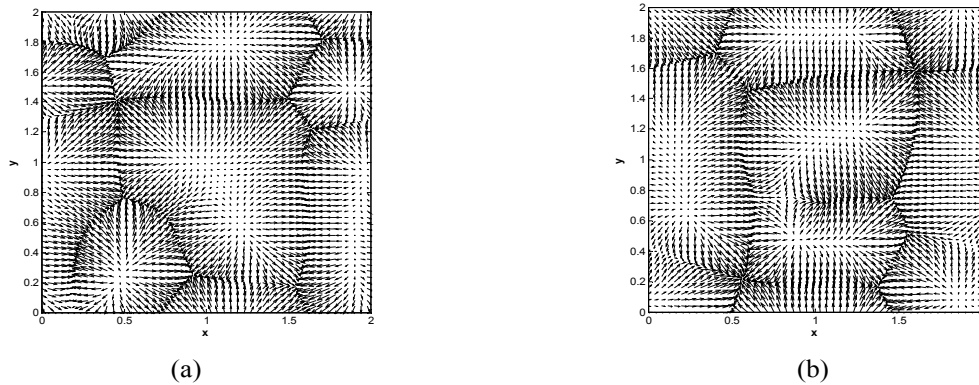
The flow pattern for  $A=2$  is again a single square cell. For  $A=3$  the result is different – inclined square cells with a size equal to the pattern size in the case  $A=2$ . The picture for  $A=4$  is drastically changed: the flow patterns are stable four rolls (Fig. 5, (right)) with hardly seen in Figure 5 (left) variable thickness chess positioned. This effect can be seen from the density plot at the middle plane  $z=0.5$  in Fig. 6 (left). In order to keep this configuration stable the velocity field is structured in a complicated way illustrated in Fig. 6 (right) with the  $xy$ -velocity field at  $z=0.5$ . Here one can observe a stable low intensity secondary flow in  $xy$ -directions.



**FIGURE 6.** The density field at  $z=0.5$  (left) and the 3D velocity vector plot (right) for  $Kn=0.02$ ,  $A=4$ .

The analysis of the flow patterns obtained by DSMC simulations for  $Kn=0.02$  leads to following two conclusions. First, the flow configuration depends strongly on the boundary conditions and the aspect ratio. Thus, for the small aspect ratio  $A=2$  we have a single square cell for all magnitudes of  $Fr$  ranged within the zone of convection. For  $A=3$  the patterns are the same in form and size but are inclined. Similar inclined patterns have obtained by Watanabe [3] for odd aspect ratios. This can be explained with the link between the periodicity boundary conditions and the odd aspect ratio. Second, there are long ranged correlations which are cut-off in the small aspect ratio computations. This conclusion is supported by the results shown in figures 5 and 6. The case with  $A=4$  shows that the larger computational box allows four roll configuration; this is not observed in the cases with  $A=2.0$  and  $A=3.0$ .

Figures 7 (a) – (f) present a case of chaotic Rayleigh-Bénard convection at  $Kn=0.002$ ,  $Fr=1.0$ , and  $r=0.1$ , obtained by using Navier-Stokes calculations. The series of snapshots taken at different times after the end of the transient period illustrates the time evolution of the convection patterns within a period of about 100 units in the chosen time scale. The times are selected in a way that the  $xy$ -velocity vector fields at a fixed  $z=0.9$  (close to the cold wall) show a variety of typical flow patterns. Most of them are in the form of unstable polygonal configurations interacting with each other in a complicated way. In the figures the narrow stripes with gathering arrows of the velocity vectors delineate the edges of the polygons where the cold flux goes down from the cold (top) to the hot (bottom) wall. Within a wide area inside the polygons the flux is directed up. The size of the configurations varies from small flow patterns (Fig. 7 (c)) less than  $1/10$  of the computational box size to large ones (Fig. 7 (e)) comparable to it.



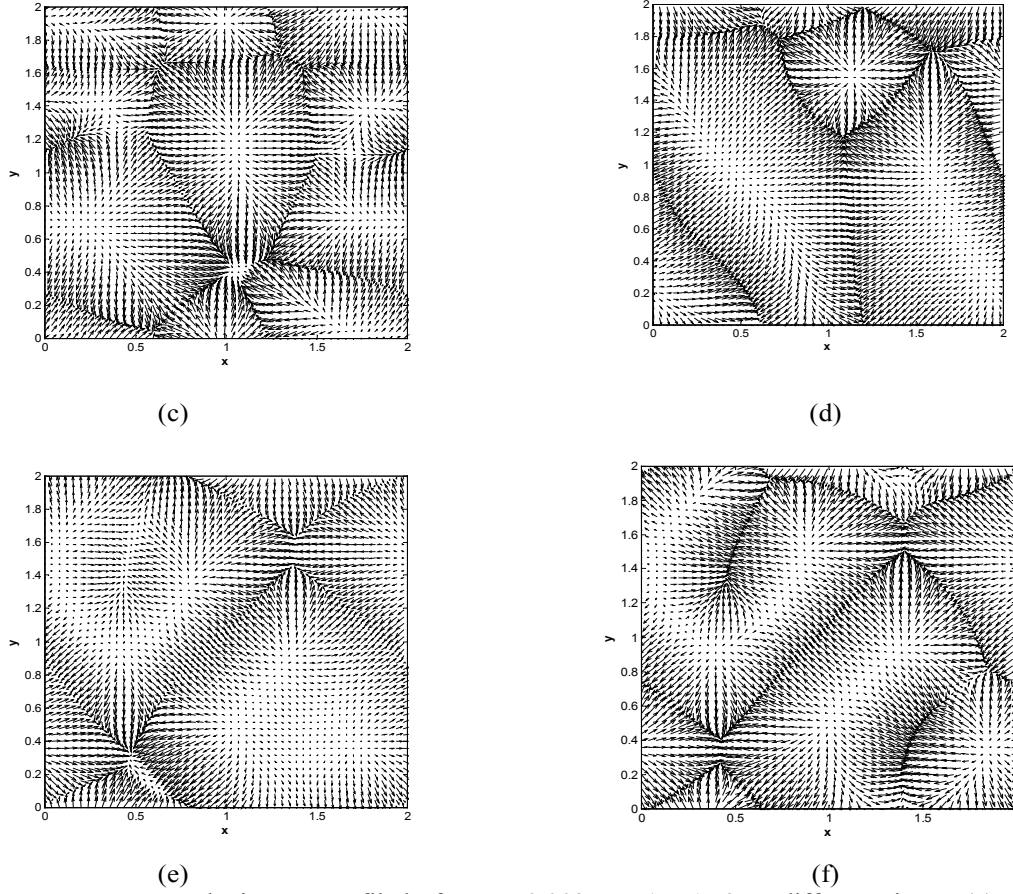


**FIGURE 7.** Instantaneous velocity vector field for  $Kn=0.002$ ,  $Fr=1$ ,  $A=2$  at different times: (a)  $t=200.0$ ; (b)  $t=220.0$ ; (c)  $t=235.0$ ; (d)  $t=260.0$ ; (e)  $t=280.0$ ; (f)  $t=300.0$ .

## ACKNOWLEDGMENTS

The research described in this paper was supported by MURST of Italy and the Bulgarian Ministry of Education and Sciences.

## REFERENCES

1. Stefanov S., Roussinov V., and Cercignani C., Phys. Fluids 14, 2255-2269 (2002).
2. Stefanov S., Roussinov V., and Cercignani C., Phys. Fluids 14, 2270-2288 (2002).
3. Watanabe T., and Kaburaki H., Phys. Rev. E 56, 1218-1221 (1997).
4. Garcia A., and Penland C., J. Stat. Phys. 64, 1121-1132 (1991).
5. Watanabe T., Kuburaki H., and Yokokawa M., Phys. Rev. E 49, 4060-4064 (1994).
6. Stefanov S. and Cercignani C., Eur. J. Mech. B/Fluids 11, 543-554 (1992).
7. Sone Y., Aoki K., and Sugimoto H., Phys. Fluids 9, 3898-3914 (1997).
8. Bird G., Molecular Gas Dynamics and the Direct Simulation of Gas Flows, Clarendon, Oxford, 1994.